A Nature-Inspired Feature Selection Approach based on Hypercomplex Information

Gustavo H. de Rosa, João P. Papa
Department of Computing
São Paulo State University
Bauru, São Paulo - Brazil
gustavo.rosa@unesp.br, joao.papa@unesp.br

Xin-She Yang
School of Science and Technology
Middlesex University
London, United Kingdom
x.yang@mdx.ac.uk

January 15, 2021

Abstract

Feature selection for a given model can be transformed into an optimization task. The essential idea behind it is to find the most suitable subset of features according to some criterion. Nature-inspired optimization can mitigate this problem by producing compelling yet straightforward solutions when dealing with complicated fitness functions. Additionally, new mathematical representations, such as quaternions and octonions, are being used to handle higher-dimensional spaces. In this context, we are introducing a meta-heuristic optimization framework in a hypercomplex-based feature selection, where hypercomplex numbers are mapped to real-valued solutions and then transferred onto a boolean hypercube by a sigmoid function. The intended hypercomplex feature selection is tested for several meta-heuristic algorithms and hypercomplex representations, achieving results comparable to some state-of-the-art approaches. The good results achieved by the proposed approach make it a promising tool amongst feature selection research.

Keywords Meta-heuristic optimization · Hypercomplex spaces · Feature selection

1 Introduction

Optimization techniques became more and more popular in the last few years. Beneficial in numerous applications, ranging from engineering [1, 2], medicine [3, 4] to machine learning fine-tuning [5, 6, 7, 8], they provide suitable solutions and virtually none human interaction with the modeling process, leaving the burden of choosing parameters to the model itself. In this context, most of the obstacles described by non-convex mathematical functions [9] requires more robust optimization approaches rather than conventional optimization methods.

Meta-heuristics algorithms, usually referred to as nature-inspired, or even to swarm- or evolutionary-based algorithms, gained great attention in the last years, attempting to solve optimization problems in a more appealing way than traditional methods. These so-called nature techniques work without derivatives, thus being suitable for problems with high dimensional spaces. Even though they provide outstanding results in different applications, they can still get trapped into local optimal points. Thus, an important question is how to run these algorithms in the case of complex objective functions. One can refer to hybrid variants [10], aging mechanisms [11], and fitness landscape analysis [12] as some distinct strategies used to deal with this issue.

As mentioned above, the problem of selecting possible parameters can be solved as an optimization problem, where a subset of parameters or features can be used to calculate the value of a fitness function. This is similar to feature selection, and it is usually classified into two divisions: (i) wrapper approaches [13], and (ii) filter-based [14]. The former methods use the output of some classifier (e.g., classification accuracy) to control the optimization method. Conversely, filter-based ones do not consider this information.

One can presume that feature selection is a straightforward solution that automatizes the choice of parameters. However, it is still necessary to select an appropriate fitness function, which is regularly correlated to the problem's nature. Also, most machine learning problems deal with high-dimensional data, thus amplifying the problem of exploring the search space. An intriguing way to tackle this obstacle is to use a more complex representation of the search space, the so-called hypercomplex search space. The goal behind handling hypercomplex spaces is based on the possibility of having more natural fitness landscapes, although it has not been mathematically proved yet. Nevertheless, the results achieved previously sustain such a hypothesis [15, 16, 17, 18].

Normalized quaternions, also known as versors, are broadly used to describe the orientation of objects in three-dimensional spaces, being extremely efficient in performing rotations in such spaces [19]. Another intriguing addition of quaternions are the octonions, comprised of eight dimensions [20]. Even though they are not well known in the literature, they have compelling traits that make them suitable for special relativity and quantum mechanics, among other research specialties [21, 22]. However, to the best of our knowledge, they have not been used to embed search spaces in meta-heuristic feature selection so far.

This study considers 8 meta-heuristic techniques, among with their quaternion- and octonion-based versions, validated under 20 different datasets, proving the robustness of quaternionic and octatonic representations for hypercomplex-embedded search spaces. Therefore, we believe this paper can serve as a foundation for prospective research regarding hypercomplex representations in the context of meta-heuristic-based feature selection.

The rest of this paper is organized as follows. Sections 2 and 3 present the theoretical background related to hypercomplex-based spaces (quaternions and octonions), and the proposed approach for hypercomplex-based feature selection, respectively. Section 4 discusses the methodology and the computational setup adopted in this paper, while Section 5 presents the numerical results. Finally, Section 6 states conclusions and future works.

2 Hypercomplex-based Spaces

2.1 Complex Numbers

The following problems can be solved with the modern methods of numerical analysis:

$$x^2 + 1 = 0, \tag{1}$$

in spite of the fact that $x^2 = -1$ cannot be a rational solution as any number square root must be positive, $x \in \Re$.

The problem (1) can be solved using the imaginary representation:

$$i^2 = -1, \tag{2}$$

although this may not appear to be logically correct. The imaginary numbers assemble a structure called *complex numbers*, which is formed by real and imaginary terms, as follows:

$$c = h_0 + h_1 i, \tag{3}$$

where $h_0, h_1 \in \Re$ and $i^2 = -1$. One can perceive that it is feasible to obtain a real number by using $h_1 = 0$, or even an imaginary number by placing $h_0 = 0$. Thus, the complex numbers deal with the generalization of both real and imaginary numbers.

One striking operation that performs positively well in a two-dimensional space is the rotation of complex numbers. Firstly, let us map a complex number on a two-dimensional grid, called *complex plane*, where the horizontal axis holds the real part mapping (**Re**), and the vertical axis is accountable for the imaginary part (**Im**). This description is depicted by Figure 1.

One can see that we need to multiply a complex number by i for each 90-degree rotation in the complex plane. To clarify this, let us consider a random point denoted by $r = i + 1$. Also, let x be the result of the multiplication of r by i, as follows:

$$x = ri = i + i^2 = -1 + i. \tag{4}$$

Now, we can obtain a singular y point by multiplying again x by i:
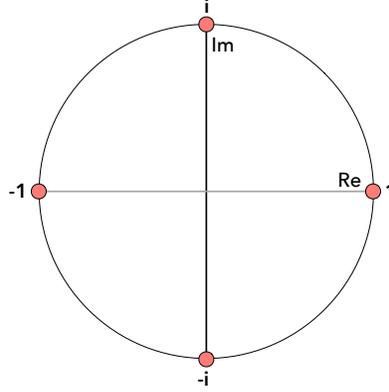
$$y = xi = -i + i^2 = -1 - i. \tag{5}$$

Figure 1: Representation of a complex plane, which is used to map complex numbers onto a two-dimensional space.

Moreover, if we multiply the result y by i, a w point can be achieved as follows:

$$w = yi = -i - i^2 = 1 - i. \tag{6}$$

Finally, by multiplying w with i, we conclude:

$$z = wi = i - i^2 = 1 + i, \tag{7}$$

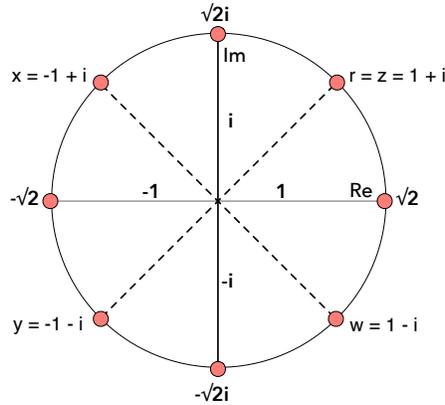where z is the same first defined position, i.e., $r = z$. Figure 2 illustrates the above calculations.

Figure 2: Representation of complex numbers' rotation throughout the complex plane.

2.2 Hypercomplex Numbers

In a particular behavior, we can extend the idea of complex numbers by adding new imaginary terms, producing the so-called hypercomplex numbers. This concept also allows rotations to be performed in higher-dimensional complex spaces. In this work, we consider two traditional hypercomplex representations: quaternions and octonions.

2.2.1 Quaternions

A quaternion q is a hypercomplex number, composed of real and complex parts, being $q = h_0 + h_1 i + h_2 j + h_3 k$, where $h_0, h_1, h_2, h_3 \in \Re$ and i, j, k are imaginary numbers (also known as "fundamental quaternions units"). This assumption is hold by the following set of equations:

$$ij = k, \tag{8}$$

3

$$jk = i, \tag{9}$$

$$ki = j, \tag{10}$$

$$ji = -k, \tag{11}$$

$$kj = -i, \tag{12}$$

$$ik = -j, \tag{13}$$

and

$$i^2 = j^2 = k^2 = -1. \tag{14}$$

Essentially, a quaternion q is a four-dimensional space representation over the real numbers, i.e., $\Re^4$.

Given two arbitrary quaternions $q_1 = g_0 + g_1 i + g_2 j + g_3 k$ and $q_2 = h_0 + h_1 i + h_2 j + h_3 k$, the quaternion algebra defines a set of main operations [23]. The addition operation, for instance, can be defined as follows:

$$\begin{aligned} q_1 + q_2 &= (g_0 + g_1 i + g_2 j + g_3 k) + (h_0 + h_1 i + h_2 j + h_3 k) \\ &= (g_0 + h_0) + (g_1 + h_1)i + (g_2 + h_2)j + (g_3 + h_3)k, \end{aligned} \tag{15}$$

while the subtraction is defined as follows:

$$\begin{aligned} q_1 - q_2 &= (g_0 + g_1 i + g_2 j + g_3 k) - (h_0 + h_1 i + h_2 j + h_3 k) \\ &= (g_0 - h_0) + (g_1 - h_1)i + (g_2 - h_2)j + (g_3 - h_3)k. \end{aligned} \tag{16}$$

Morever, Fister et al. [15, 16] introduced two other operations, q_{rand} and q_{zero}. The former initializes a given quaternion with values drawn from a Gaussian distribution $\mathcal{N}$, and is defined as follows:

$$q_{\text{rand}}() = \{g_i = \mathcal{N}(0, 1) \mid i \in \{0, 1, 2, 3\}\}. \tag{17}$$

The latter equation initializes a quaternion with zero values, as follows:

$$q_{\text{zero}}() = \{g_i = 0 \mid i \in \{0, 1, 2, 3\}\}. \tag{18}$$

2.2.2 Octonions

Octonions are a natural extension of quaternions and were discovered autonomously by John T. Graves and Arthur Cayley around 1843. An octonion is composed of seven complex parts and one real-valued term, being defined as follows:

$$o = h_0 e_0 + h_1 e_1 + h_2 e_2 + \ldots + h_7 e_7, \tag{19}$$

where $h_i \in \Re$ and e_i are the imaginary numbers, $i = 0, \ldots, 7$. Commonly, $e_0 = 1$ is used in order to obtain the real-valued term of the octonion.

The addition, subtraction, and norm equations are computed likewise to the quaternions' formulae, giving us a clear implementation framework in order to manipulate several hypercomplex representations.

3 Feature Selection

This section outlines the proposed method for meta-heuristic-based feature selection. One can understand the feature selection process as a method that decides whether a feature should be selected or not (boolean) in order to solve a given problem. As traditional optimization algorithms use a continuous-valued search space, we need to shape the search space into an n-dimensional binary structure, where solutions are selected across the edges of a hypercube. Furthermore, as our problem is to select or not a feature, each solution individual is now an n-dimensional binary array, where each dimension corresponds to a specific feature and the values 1 and 0 indicate whether this feature will or will not be part of the new set.

Concerning conventional optimization algorithms, the solutions are found upon continuous-valued positions of the search space. In order to accomplish this binary-valued individual, one can restrain the new solutions to binary values only:

$$S(x_i^j) = \frac{1}{1 + e^{-x_i^j}}, \tag{20}$$

$$x_i^j = \begin{cases} 1 & \text{if } S(x_i^j) > \alpha, \\ 0 & \text{otherwise} \end{cases} \tag{21}$$

in which $\alpha \sim U(0,1)$, and $x \in \Re$ stands for a possible solution.

Equation 20 represents the *transfer function*, which maps real-valued solutions into binary-valued ones. Note that any transfer functions can be used to fulfill this purpose. In this work, we are using a sigmoid function (Equation 20), which is illustrated by Figure 3 to map bounded real-valued solutions[1] is bounded within the interval $[-20, 20]$. and generate a probability. Further, the mapped value is compared against a uniform distribution sampling in order to obtain the binary output (Equation 21).
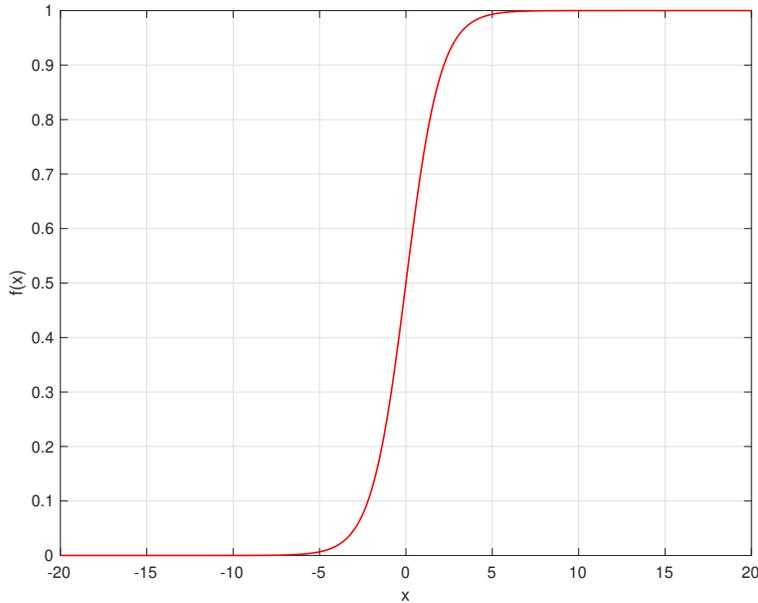

Figure 3: Sigmoid transfer function $f(x) = \frac{1}{1+e^{-x}}$ bounded in $[-20, 20]$.

3.1 Hypercomplex Feature Selection

A hypercomplex-based feature selection strategy does not deviate too much from the regular method. One can encode the common search space into a higher-dimensional space, by applying the power of quaternions or octonions. When

---

[1]Each real-valued solution

conducting the meta-heuristic algorithm through the hypercomplex space towards a feasible solution, a crucial operator that needs to be defined is the p-norm, which is responsible for mapping hyper-complex values to real numbers. Let q be a hypercomplex number with real coefficients $\{h_d\}_{d=1}^{D}$, one can compute the Minkowski p-norm as follows:

$$\|q\|_p = \left(\sum_{d=1}^{D} |h_d|^p\right)^{1/p} \tag{22}$$

where D is the number of dimensions of the space (2 for complex numbers, 4 for quaternions and 8 for octonions, for instance) and $p \geq 1$. Common values for the latter variable are 1 or 2 for the Taxicab and Euclidean[2] norms, respectively. Hence, one can see the p-norm as a generalization of such distance operators.

Prior to the transfer function activation, there is an additional equation, called the Span function, which is responsible for mapping the norm's output between the lower and upper bounds, as follows:

$$q_{span}() = (b_u - b_l)\frac{\|q\|_p}{D^{1/p}} + b_l, \tag{23}$$

where b_l and b_u stands for the lower and upper bounds, respectively.

Figure 4 illustrates an encoding of a solution vector $\boldsymbol{x}$ into a quaternionic space, where x_i^j depicts the i-th component of the hypercomplex number for the j-th decision variable. The same approach can be applied to octatonic spaces by extending the quaternion q (four components) to an octonion o (eight components).

Figure 4: Quaternionic hypercomplex encoding of a solution vector $\boldsymbol{x}$, such that x_i^j stands for the i-th component of the hypercomplex number for the j-th decision variable.

4   Methodology and Setup

The idea behind this work is to model the task of selecting the most suitable features for a given problem through a meta-heuristic optimization process. As stated in Section 1, feature selection stands for a proper selection of features, reducing a particular problem's dimensionality and usually enhancing its performance. Also, as the proposed approach is a wrapper-based one, there is a need to define an objective function that will conduct the optimization process. Therefore, the proposed approach aims at selecting the subset of features that minimize the classification error (maximize the classification accuracy) of a given supervised classifier over a validation set. Although any supervised pattern recognition classifier could be applied, we opted to use the Optimum-Path Forest (OPF) [24, 25] since it is parameterless and has a fast training procedure. Essentially, the OPF encodes each dataset's sample as a node in a graph, whose connections are defined by an adjacency relation. Its learning process aims at finding prime samples called *prototypes* and trying to conquer the remaining samples by offering them optimum-paths according to a path-cost function. In the end, optimum-path trees are achieved, each one rooted at a different prototype node.

---

[2]In this work, we opted to use the Euclidean Norm as mapping function.

Dataset	Task	# Training Samples	# Testing Samples	# Features
Arcene	Mass Spectrometry	100	100	10,000
BASEHOCK	Text	997	996	4,862
COIL20	Face Image	770	770	1,024
DNA	Biological	2,000	1,186	180
Isolet	Spoken Letter Recognition	780	780	617
Lung	Biological	102	101	3,312
Madelon	Artificial	2,000	600	500
MPEG7-BAS	Image Descriptor	700	700	180
MPEG7-Fourier	Image Descriptor	700	700	126
Mushrooms	Biological	4,062	4,062	112
NTL-Commercial	Energy Theft	2,476	2,476	8
NTL-Industrial	Energy Theft	1,591	1,591	8
ORL	Face Image	200	200	1,024
PCMAC	Text	972	971	3,289
Phishing	Network Security	5,528	5,527	68
Segment	Image Segmentation	1,155	1,155	19
Sonar	Signal	104	104	60
Splice	Biological	1,000	2,175	60
Vehicle	Image Silhouettes	423	423	18
Wine	Chemical	89	89	13

Table 1: Employed datasets used in the computations

.

Given a set of hypercomplex candidate solutions $\{\boldsymbol{s}\}_{i=1}^{S}$, where $\boldsymbol{s} = \{s_1, s_2, \ldots, s_j\} \mid j \in \{1, 2, \ldots, N\}$, such that S stands for meta-heuristic candidates and N for the number of decision variables (number of the problem's features depicted in Table 1), we wish to learn the best set of features $F^{\star}$. Namely, we want to solve the following optimization problem:

$$F^{\star} = \{f_i(\boldsymbol{s}_i, F) \mid i \in [1, S]\},$$
$$\text{st. } 1 \leq F \leq N. \tag{24}$$

where $f_i(\boldsymbol{s}_i, F)$ stands for the fitness function (OPF accuracy over validation set) of candidate i based on its binary solution $\boldsymbol{s}_i$, which is responsible for activating or deactivating the set of features F. Finally, the meta-heuristic intrinsic mechanics[3] are executed to identify the best solution so far and to update the candidates' position in the hypercomplex space.

4.1 Datasets

Table 1 describes all the datasets utilized in this work. We selected 20 datasets that diversify within the number of samples, classes, and features, suggesting a more strong validation under distinguished scenarios. The datasets were downloaded from LibSVM's project[4] and Arizona State University's (ASU) repository[5], being already quantized for categorical features and processed for missing values[6]. As we need a unique set to guide the optimization process, not being the test one, we partitioned all datasets' training sets in half, composing the so-called validation set. Therefore, we use 25% for the training step, 25% for the optimization task validation, and the remaining 50% to assess the experimental validation (testing step).

---

[3]Note that some meta-heuristic might start their searching procedure with every possible initial features, while others might start with a randomly subset of the initial features.

[4]https://www.csie.ntu.edu.tw/c̄jlin/libsvmtools/datasets

[5]http://featureselection.asu.edu/datasets.php

[6]One can find their post-processed versions at: http://recogna.tech

Algorithm	Parameters
ABC	number of trials $= 1,000$
AIWPSO	$c_1 = 1.7 \mid c_2 = 1.7 \mid w = [0.5, 1.5]$
BA	$f = [0, 100] \mid A = 1.5 \mid r = 0.5$
CS	$\beta = 1.5 \mid p = 0.25 \mid \alpha = 0.8$
FA	$\alpha = 0.2 \mid \beta = 1.0 \mid \gamma = 1.0$
FPA	$\beta = 1.5 \mid p = 0.8$
PSO	$c_1 = 1.7 \mid c_2 = 1.7 \mid w = 0.7$

Table 2: Parameter settings for the meta-heuristic algorithms considered in the work.

4.2 Computational Setup

The source code used in this work comes from two libraries: LibOPT[7] and LibDEV[8]. Both libraries are implemented in the C language and have been extensively used throughout scientific research. The LibOPT library is a collection of meta-heuristic optimization techniques, while the LibDEV library provides an integration environment, e.g., feature selection conducted over meta-heuristic optimizations. One can refer to [26] in order to understand how it is possible to work under the LibOPT environment, i.e., how to design a hypercomplex optimization task.

To perform a reasonable comparison among distinct meta-heuristic techniques, we must rely on mathematical methods that will sustain these observations. The first step is to decide whether to use a parametric or a non-parametric statistical test [27]. Unfortunately, we can not consider a normality state from our numerical trials due to the aleatory and non-deterministic factor derived from the meta-heuristic techniques, restraining our analysis to non-parametric approaches.

Secondly, acknowledging that the results of our numerical trials are independent (i.e., classification accuracy) and continuous over a particular dependent variable (i.e., number of observations), we can identify that the Wilcoxon signed-rank test [28] will satisfy our obligations. It is a non-parametric hypothesis test used to compare two or more related observations (in our case, repeated measurements over a certain meta-heuristic) to assess whether there are statistically significant differences between them.

For every dataset, each meta-heuristic was evaluated under a 2-fold cross-validation[9] with 25 runs. Additionally, for every meta-heuristic, 15 agents (particles) were used over 25 convergence iterations. To provide a thorough comparison between meta-heuristics, we have chosen different techniques, ranging from swarm-based to evolutionary-inspired ones, in the context of feature selection:

- Artificial Bee Colony (ABC) [29];
- Adaptive Inertia Weight Particle Swarm Optimization (AIWPSO) [30];
- Bat Algorithm (BA) [31];
- Cuckoo Search (CS) [32];
- Firefly Algorithm (FA) [33];
- Flower Pollination Algorithm (FPA) [34];
- Particle Swarm Optimization (PSO) [35].

Note that, for each selected meta-heuristic, we will also present their quaternion- and octonion-based versions, being the former preceded by a Q prefix and the latter preceded by an O prefix. Table 2 presents the chosen parameter setting for every meta-heuristic technique[10]. We overlooked quaternion- and octonion-based algorithms from the table, as their parameters are the same as their original version.

Concerning ABC, we only need to set the number of trial limits for each food source. AIWPSO defines minimum and maximum weight as a w interval, and c_1 and c_2 as the control parameters. BA has the minimum and maximum

---

[7]https://github.com/jppbsi/LibOPT

[8]https://github.com/jppbsi/LibDEV

[9]Remember that the training set was again split in half to form the validation set, used during the optimization process.

[10]Note that these values were empirically chosen according to their authors' definition.

frequency ranges defined by f interval, as well as the loudness parameter A and pulse rate r. With CS, we demand to set up β, which is used to compute the Lévy distribution, as well as p, which is the probability of replacing worst nests by new ones and α which is the step size. Regarding FA, we have α for calculating the randomized parameter, as well as the attractiveness parameter β_0 and the light absorption coefficient γ. FPA requires the β parameter, used to compute the Lévy distribution and p, which is the probability of local pollination. Finally, PSO defines w as the inertia weight, and c_1 and c_2 as the control parameters.

5 Numerical Results

This section presents the numerical results concerning the proposed experiments. Furthermore, it is divided into two subsections, which are in charge of discussing the overall analysis and the convergence analysis, respectively.

In order to provide statistical analysis to the numerical results, we opted to bold the best results' cells according to the Wilcoxon signed-rank test with 5% of significance. In other words, it is possible to observe that, regarding a particular column, every bolded cell achieved the most suitable accuracy, time, or number of features according to the statistical test.

5.1 Overall Analysis

Table 3 describes all datasets' average accuracy over the test set found by each meta-heuristic technique. A very interesting fact to highlight is that for almost every dataset, at least one meta-heuristic technique was able to achieve a performance comparable to the baseline approach, i.e., OPF classification using the whole dataset. On the other hand, considering Arcene, Mushrooms, NTL-Commercial, NTL-Industrial, and Splice datasets, meta-heuristic techniques outperformed the baseline approach.

Regarding only meta-heuristic techniques and their hypercomplex versions, one can see that the hypercomplex-based algorithms were able to achieve comparable accuracy values. In some cases, they even outperformed their naïve versions, e.g., QFA, QFPA, OFPA, and QPSO on Arcene; QAIWPSO on COIL20; QAIWPSO on Madelon; QCS, QFPA, and OFPA in Mushrooms; QABC and OABC in ORL; QABC, QBA, and OBA in PCMAC; QABC, OABC, OAIWPSO, QFA, OFA, QFPA and OFPA in Phishing; OABC and QPSO in Splice; QCS and OCS in Wine. In such case, outperforming means that a particular technique was capable of achieving a higher accuracy than another technique. Essentially, the Wilcoxon signed-rank test assess whether there was a statistical similarity between the accuracies obtained by each one of the techniques. Thus, as the statistical test was conducted over the independent accuracies for each meta-heuristic technique, it is possible to observe that the most significant techniques (bolded ones) in the aforementioned cases were also the ones that achieved higher accuracy than their naïve versions.

	ABC	QABC	OABC	AIWPSO	QAIWPSO	OAIWPSO	BA	QBA	OBA	CS	QCS	OCS	FA	QFA	OFA	FPA	QFPA	OFPA	PSO	QPSO	OPSO	BASELINE
Arcene	**83.13%**	83.04%	**83.13%**	**83.50%**	82.89%	82.52%	82.83%	82.72%	82.61%	82.41%	82.38%	82.75%	82.70%	**83.04%**	82.55%	82.72%	**82.90%**	**82.92%**	82.26%	**83.21%**	82.47%	81.58%
BASEHOCK	79.49%	79.07%	79.98%	79.67%	79.86%	78.84%	79.99%	79.58%	79.73%	80.14%	78.87%	79.83%	79.25%	79.99%	79.62%	79.80%	79.00%	79.02%	79.63%	79.59%	80.13%	**82.12%**
COIL20	99.04%	99.09%	99.03%	99.02%	**99.13%**	99.07%	99.09%	99.08%	99.08%	**99.12%**	99.09%	99.07%	99.08%	99.06%	99.09%	99.09%	99.04%	99.10%	**99.13%**	99.07%	99.04%	**99.30%**
DNA	79.43%	79.58%	79.17%	78.95%	78.70%	78.64%	79.08%	79.32%	77.55%	77.90%	77.49%	78.06%	78.69%	79.23%	78.97%	79.17%	79.30%	79.30%	79.51%	78.71%	79.26%	**82.33%**
Isolet	90.79%	90.81%	90.72%	90.89%	90.77%	90.83%	90.55%	90.71%	90.77%	90.57%	90.71%	90.70%	90.68%	90.89%	90.73%	90.77%	90.67%	90.69%	90.67%	90.71%	90.66%	**91.30%**
Lung	93.08%	**93.13%**	92.68%	91.95%	92.43%	92.26%	92.61%	92.66%	92.77%	92.20%	92.47%	92.56%	92.70%	92.54%	92.49%	92.88%	92.71%	92.87%	92.83%	91.89%	92.51%	**93.24%**
Madelon	63.42%	62.69%	63.00%	62.73%	**64.52%**	63.21%	**63.85%**	62.25%	**65.12%**	63.48%	62.69%	**63.63%**	**63.94%**	63.23%	62.79%	62.81%	**63.70%**	63.41%	62.87%	63.03%	62.47%	**64.37%**
MPEG7-BAS	88.78%	**88.85%**	88.90%	88.91%	88.90%	88.90%	88.80%	**88.98%**	88.81%	**88.92%**	**88.97%**	88.81%	88.89%	**88.99%**	88.83%	88.81%	**88.85%**	88.81%	**88.90%**	**88.96%**	88.88%	**89.11%**
MPEG7-Fourier	**72.12%**	71.94%	72.00%	71.91%	71.91%	**72.18%**	**72.19%**	72.06%	**72.18%**	69.46%	70.00%	70.49%	71.78%	71.86%	**71.96%**	**72.02%**	**72.19%**	72.16%	72.12%	**72.22%**	72.14%	72.09%
Mushrooms	96.19%	96.57%	**98.81%**	96.61%	97.63%	97.43%	95.81%	96.61%	94.04%	97.11%	**97.40%**	94.62%	**96.90%**	94.80%	96.31%	94.14%	95.68%	**97.09%**	96.09%	95.39%	96.09%	94.36%
NTL-Commercial	**92.73%**	92.59%	92.16%	91.84%	90.78%	92.39%	92.42%	92.17%	91.93%	79.22%	76.07%	79.99%	91.71%	91.99%	92.05%	92.17%	92.39%	91.76%	92.52%	**92.57%**	91.93%	61.45%
NTL-Industrial	95.77%	95.36%	95.31%	95.40%	95.37%	95.42%	**95.58%**	95.04%	95.22%	77.90%	82.95%	79.16%	94.80%	**95.82%**	94.64%	95.05%	94.79%	94.77%	94.99%	94.84%	94.54%	67.86%
ORL	93.56%	**93.75%**	93.60%	93.67%	93.54%	93.46%	93.57%	93.84%	93.57%	93.62%	93.60%	93.53%	93.58%	93.60%	93.69%	93.66%	93.56%	93.72%	**93.75%**	93.57%	93.49%	93.25%
PCMAC	71.97%	**72.24%**	71.35%	**72.44%**	71.16%	71.58%	71.18%	**71.83%**	**73.18%**	72.03%	**72.32%**	71.98%	71.99%	71.50%	72.19%	**72.78%**	72.54%	72.36%	71.81%	71.64%	**72.35%**	72.75%
Phishing	84.53%	**85.36%**	**86.56%**	84.74%	84.02%	**85.99%**	84.92%	85.49%	**84.76%**	85.40%	84.90%	84.06%	83.35%	**85.26%**	85.19%	84.40%	**84.40%**	**85.61%**	84.79%	84.10%	**85.93%**	86.67%
Segment	97.33%	97.19%	97.25%	97.15%	97.05%	97.20%	97.19%	97.20%	97.06%	96.22%	96.35%	95.95%	97.29%	96.82%	97.21%	97.13%	97.20%	97.19%	97.17%	**97.31%**	96.83%	**97.34%**
Sonar	79.40%	**81.72%**	79.57%	**81.21%**	**81.56%**	79.89%	**81.20%**	80.15%	80.62%	80.44%	**80.94%**	80.76%	80.32%	80.20%	80.76%	79.80%	**80.53%**	80.80%	80.78%	80.14%	80.77%	81.75%
Splice	71.64%	71.33%	**71.99%**	71.87%	**71.72%**	70.99%	70.93%	71.14%	71.32%	69.53%	69.56%	70.21%	**71.32%**	71.33%	71.50%	**72.30%**	**71.83%**	71.08%	70.81%	**71.68%**	71.35%	70.89%
Vehicle	78.17%	77.41%	77.62%	77.11%	77.25%	**77.42%**	**77.60%**	77.51%	76.98%	76.74%	76.20%	76.34%	77.25%	76.79%	77.11%	**77.46%**	77.09%	**77.71%**	76.93%	76.53%	76.85%	**77.63%**
Wine	96.21%	96.46%	**96.58%**	95.94%	95.62%	**95.96%**	**96.67%**	96.63%	96.23%	94.87%	**95.51%**	**95.55%**	96.42%	96.22%	95.99%	96.16%	96.09%	95.81%	96.23%	96.39%	95.98%	95.80%

Table 3: Average accuracy achieved over the test set considering all datasets.

An interesting fact emerging from Table 4 is that CS was able to achieve the lowest number of features in nearly every dataset. Furthermore, when standard CS did not deliver the lowest number of features, its quaternionic and octatonic representations were able to achieve this intent[11].

Even though most algorithms were able to diminish the features' space size and obtain statistically similar accuracy within respect to the baseline method, in some cases they reached a slightly lower accuracy than the original OPF classification. However, it should be noted that in the case of the BASEHOCK dataset, where even the baseline classification obtained the best accuracy, all other meta-heuristic techniques could reduce by about 35% of the number of features while scoring 2-3% lower accuracy than OPF.

	ABC	QABC	OABC	AIWPSO	QAIWPSO	OAIWPSO	BA	QBA	OBA	CS	QCS	OCS	FA	QFA	OFA	FPA	QFPA	OFPA	PSO	QPSO	OPSO	BASELINE
Arcene	6462.88	6473.48	6482.36	6454.20	6492.80	6467.04	6476.72	6486.52	6512.96	**6419.40**	6453.76	6478.40	6466.00	6471.68	6491.80	6471.56	6481.52	6479.60	6450.84	6468.56	6505.52	10000.00
BASEHOCK	3166.92	3141.28	3142.16	3148.48	3149.76	3153.28	3167.52	3167.60	3170.32	**3124.72**	3143.72	3139.64	3152.16	3146.40	3156.52	3151.52	3131.08	3135.00	3149.40	3147.32	3147.68	4862.00
COIL20	670.04	666.16	663.92	658.92	664.12	668.84	667.56	668.28	674.88	**654.52**	660.52	664.56	666.12	664.44	667.00	663.56	664.08	666.44	664.40	666.80	666.88	1024.00
DNA	117.04	117.48	116.44	117.20	116.80	117.88	119.96	116.92	116.72	118.04	116.36	**113.00**	117.84	116.40	115.96	119.04	117.96	119.00	115.00	116.28	117.00	180.00
Isolet	407.08	401.12	398.16	396.24	399.12	401.08	399.48	403.36	408.84	**393.40**	398.64	401.40	402.52	397.88	399.76	402.20	397.68	400.32	397.24	397.88	399.72	617.00
Lung	2138.28	2132.52	2135.64	**2125.32**	2143.64	2147.60	2148.08	2151.12	2148.36	2130.36	2144.88	2143.84	2150.40	2143.88	2143.64	2136.52	2141.64	2147.96	2134.40	2145.24	2141.92	3312.00
Madelon	324.72	**321.72**	324.40	321.96	322.44	324.44	324.00	327.44	330.36	325.16	324.24	324.44	325.84	328.80	323.16	324.68	323.48	327.56	324.64	323.92	324.00	500.00
MPEG7-BAS	118.12	120.80	119.00	118.40	120.12	119.84	118.56	121.52	120.44	**115.88**	116.84	116.80	120.92	117.68	119.20	118.32	118.92	117.88	117.88	118.52	119.44	180.00
MPEG7-Fourier	81.08	82.08	81.88	82.52	**81.04**	82.36	84.36	84.40	83.08	81.12	81.48	82.64	82.64	82.92	81.24	82.36	82.84	83.04	83.88	82.44	81.32	126.00
Mushrooms	74.92	70.36	70.56	72.48	74.04	73.28	73.44	72.88	72.84	**70.32**	73.08	71.76	74.96	72.16	73.12	75.24	74.12	70.52	73.08	73.28	73.84	112.00
NTL-Commercial	5.72	5.60	5.60	5.84	5.76	5.76	5.68	5.76	5.56	5.04	5.04	**4.84**	5.68	5.72	5.44	5.64	5.68	5.64	5.68	5.48	5.44	8.00
NTL-Industrial	5.40	5.24	5.52	5.24	5.36	5.44	5.68	5.80	5.44	5.76	5.20	5.08	5.56	**5.00**	5.40	5.20	5.20	5.32	5.52	5.64	5.44	8.00
ORL	665.76	656.96	659.96	662.96	663.28	663.88	666.48	665.48	671.24	**653.92**	661.00	659.84	664.72	658.40	665.56	662.84	657.80	662.80	658.16	660.76	659.16	1024.00
PCMAC	2152.68	2114.28	2130.60	2132.16	2123.76	2128.32	2140.04	2137.88	2154.60	**2112.16**	2115.40	2123.12	2129.24	2126.48	2130.44	2135.56	2128.88	2130.92	2128.48	2126.76	2131.52	3289.00
Phishing	45.16	44.68	45.60	44.52	44.84	46.36	45.28	45.12	44.88	44.40	**44.12**	44.88	44.92	45.44	46.60	44.80	46.44	45.40	45.12	44.80	46.48	68.00
Segment	14.04	13.20	13.48	13.44	13.44	13.80	13.44	13.84	13.64	13.04	13.24	**12.40**	13.32	13.48	14.08	13.68	13.04	13.44	13.56	13.92	13.44	19.00
Sonar	40.24	39.40	38.80	39.00	39.76	40.84	40.04	37.96	39.12	39.52	39.64	39.48	**37.92**	38.24	40.28	39.76	39.08	40.32	39.48	38.24	39.96	60.00
Splice	40.48	39.72	39.72	40.68	40.24	40.28	40.56	38.80	40.64	**38.76**	39.40	40.04	39.28	40.40	40.92	40.40	39.92	40.48	40.04	40.44	39.80	60.00
Vehicle	13.40	12.68	12.72	12.84	12.00	12.28	12.60	12.96	13.40	**11.92**	12.20	12.08	12.84	12.72	13.00	13.08	13.28	12.76	13.52	12.52	13.16	18.00
Wine	9.20	9.04	9.24	**8.40**	9.04	9.12	9.28	9.00	9.56	9.04	8.80	8.88	9.04	9.08	9.48	9.00	9.32	8.76	9.28	8.92	9.48	13.00

Table 4: Average number of features used over the test set considering all datasets.

Table 5 shows that CS-based techniques completed the optimization runs in a significantly lower computation time than every other technique. Additionally, Figures 5 and 6 illustrate a more in-depth comparison between CS and its hypercomplex versions for four distinct datasets: DNA, NTL-Commercial, Phishing and Segment. One can observe that Figure 5 represents the CS-based techniques behavior, where the best techniques are positioned in the top-left corner of the graphic, i.e., best accuracy and lowest number of features. For the sake of brevity, we opted to show some datasets that have discrepant data, i.e., datasets that have a low amount of features, being more susceptible when selecting a subset of features. In such cases, any incorrect feature selection will depreciate the classification results, thus, making the convergence process more unstable.

One can perceive that CS-based techniques encountered a feasible number of features, but not necessarily the best accuracy. If one observes the difference between the best and the worst accuracy considering all datasets (except NTL-based ones) and meta-heuristic techniques, there is not a single one that surpasses the 4.77% barrier. Nevertheless, CS suffered in the NTL datasets (energy theft identification), which are highly unbalanced and have a relatively small amount of features. As CS encountered the lowest number of features in such a low-dimensional dataset, it is possible to observe that is has overfitted the optimization process to find the lowest number of possible features at the cost of penalizing the classifier, hence, achieving a not suitable accuracy for these particular datasets.

Regarding the hypercomplex techniques, such as quaternion and octonion, it is possible to observe that they have an extra computational loop per feature, due to its number of dimensions, e.g., 4 and 8. If the number of selected features is sufficiently smaller to overcome this extra loop, the hypercomplex techniques will achieve a shorter computational time than the conventional ones. For example, in a 100-features problem, the conventional technique loop lasts for 100 times, while the quaternion and octonion loops last for 400 and 800 times, respectively. If the quaternion-based technique selects 25 features averagely while the octonion-based one selects 12.5 features averagely, both will perform a loop that lasts for 100 times, being comparable to the conventional algorithm.

The results obtained in this study prove the promising use of meta-heuristic optimization techniques when selecting a quasi-optimum subset of features while preserving its performance and discriminative aptitudes.

---

[11]QCS achieved the lowest number of features for the Phishing dataset while OCS achieved this goal for the DNA, NTL-Commercial and Segment datasets.
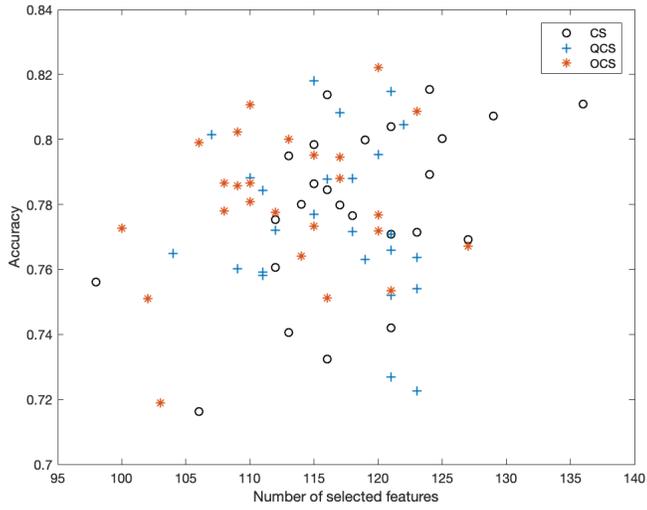
	ABC	QABC	OABC	AIWPSO	QAIWPSO	OAIWPSO	BA	QBA	OBA	CS	QCS	OCS	FA	QFA	OFA	FPA	QFPA	OFPA	PSO	QPSO	OPSO
Arcene	43.48s	42.11s	43.06s	21.59s	23.08s	23.45s	21.92s	23.97s	25.78s	**7.81s**	10.06s	11.68s	22.90s	27.62s	34.57s	22.59s	27.62s	31.83s	22.21s	22.70s	23.42s
BASEHOCK	1114.33s	1105.60s	1108.30s	563.38s	563.89s	566.88s	568.81s	571.82s	571.79s	**189.89s**	203.89s	203.53s	545.73s	543.84s	547.47s	564.81s	565.72s	567.54s	556.54s	558.63s	561.71s
COIL20	179.37s	181.11s	181.33s	90.92s	93.17s	93.01s	90.47s	92.77s	94.90s	**30.19s**	33.10s	33.57s	89.41s	88.91s	90.34s	92.62s	92.79s	94.25s	90.70s	91.86s	91.87s
DNA	240.43s	241.94s	242.54s	171.38s	171.86s	171.85s	124.60s	123.88s	123.78s	**45.01s**	46.74s	46.34s	121.66s	122.14s	122.58s	123.84s	125.02s	124.48s	171.20s	171.06s	169.50s
Isolet	135.52s	138.87s	138.42s	69.96s	70.40s	70.60s	69.60s	71.11s	71.01s	**21.85s**	25.73s	26.05s	68.44s	68.02s	69.73s	70.96s	71.09s	70.74s	68.78s	69.86s	69.86s
Lung	15.19s	15.07s	15.50s	7.84s	8.12s	8.42s	7.73s	8.60s	9.01s	**2.76s**	3.61s	4.17s	7.98s	9.61s	11.74s	7.98s	9.87s	11.24s	7.71s	7.78s	8.05s
Madelon	704.37s	698.42s	698.56s	354.86s	356.56s	357.16s	358.11s	359.54s	361.50s	**120.80s**	127.19s	128.23s	343.79s	341.46s	343.17s	355.31s	353.68s	354.26s	351.40s	352.89s	352.85s
MPEG7-BAS	38.05s	35.59s	37.25s	25.01s	25.71s	25.25s	18.78s	18.46s	18.67s	**6.61s**	7.29s	7.39s	18.96s	19.36s	19.17s	19.51s	18.89s	19.64s	25.40s	25.16s	25.06s
MPEG7-Fourier	27.92s	25.70s	25.78s	19.29s	19.54s	19.46s	13.74s	13.87s	13.97s	**4.68s**	5.00s	5.02s	13.31s	13.33s	13.25s	13.37s	13.17s	13.26s	18.91s	18.69s	18.87s
Mushrooms	791.66s	785.72s	785.15s	600.75s	600.03s	601.13s	405.80s	408.04s	409.10s	**143.20s**	151.30s	152.22s	398.83s	397.73s	398.85s	404.05s	403.06s	404.90s	597.34s	596.48s	595.58s
NTL-Commercial	272.72s	271.35s	270.80s	139.44s	138.38s	138.36s	139.15s	138.73s	138.41s	50.04s	49.76s	**49.56s**	132.70s	133.49s	133.30s	138.46s	137.85s	138.23s	138.58s	137.60s	137.83s
NTL-Industrial	113.70s	111.91s	111.74s	57.60s	56.71s	56.55s	57.79s	57.30s	57.27s	20.58s	20.62s	**20.55s**	54.88s	54.97s	54.58s	57.11s	57.30s	57.02s	57.68s	56.60s	56.46s
ORL	13.07s	13.05s	13.08s	6.73s	6.77s	6.93s	6.38s	6.96s	7.20s	**2.07s**	2.62s	2.82s	6.67s	7.56s	8.63s	6.87s	7.19s	7.67s	6.64s	6.79s	6.80s
PCMAC	751.25s	742.09s	744.23s	377.87s	381.31s	380.74s	382.81s	382.50s	386.86s	**128.28s**	136.87s	137.31s	365.66s	366.69s	370.00s	380.84s	382.02s	381.16s	374.06s	376.45s	377.26s
Phishing	1119.79s	1110.41s	1110.58s	943.66s	941.99s	939.85s	576.86s	578.64s	578.91s	**206.02s**	218.22s	218.06s	569.57s	567.55s	567.86s	574.09s	572.32s	573.75s	936.62s	933.18s	932.34s
Segment	72.41s	72.66s	72.15s	36.87s	36.99s	36.63s	37.23s	37.26s	37.11s	**13.02s**	13.43s	13.53s	35.18s	35.53s	35.46s	36.98s	37.02s	36.75s	37.25s	36.33s	36.58s
Sonar	0.51s	0.53s	0.53s	0.40s	0.41s	0.41s	0.27s	0.28s	0.29s	**0.10s**	0.11s	0.13s	0.28s	0.34s	0.41s	0.28s	0.31s	0.33s	0.40s	0.40s	0.41s
Splice	37.29s	34.84s	34.96s	30.49s	30.29s	29.83s	18.24s	18.19s	18.50s	6.94s	**6.91s**	6.99s	17.79s	17.92s	17.83s	18.33s	18.41s	18.75s	31.50s	30.83s	29.60s
Vehicle	10.01s	9.82s	9.71s	4.90s	4.93s	4.96s	4.96s	5.00s	5.04s	**1.77s**	1.79s	1.82s	4.86s	4.86s	4.89s	5.00s	5.04s	5.07s	5.02s	4.98s	4.96s
Wine	0.44s	0.44s	0.44s	0.22s	0.23s	0.23s	0.22s	0.23s	0.23s	**0.08s**	**0.08s**	0.09s	0.22s	0.23s	0.25s	0.23s	0.23s	0.24s	0.22s	0.22s	0.22s

Table 5: Average computation time required by the optimization process considering all datasets.
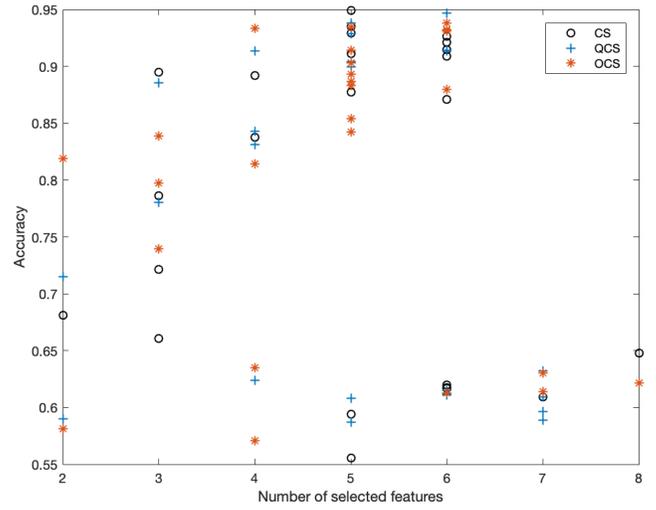
5.2 Convergence Analysis

The convergence curves of CS and its variants obtained for the DNA, NTL-Commercial, Phishing, and Segment datasets are shown in Figure 7.
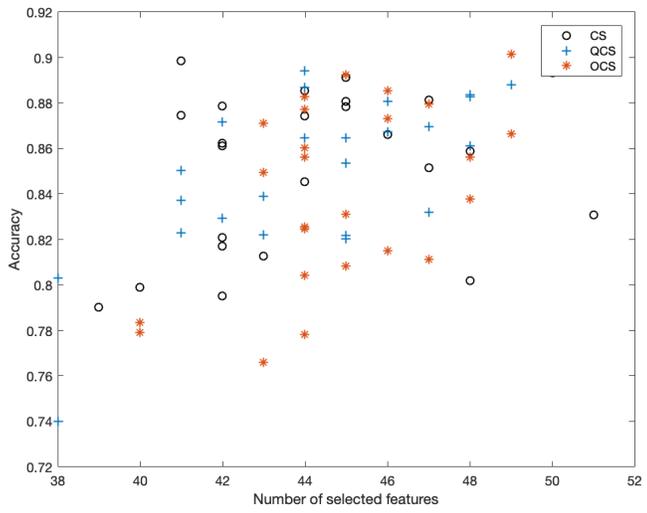
An interesting fact that one can perceive is that hypercomplex-based techniques were able to converge faster and better than the standard version in three out of four datasets (DNA, Phishing, and Segment). Additionally, it is essential to highlight that as hypercomplex-based algorithms use an enhanced version of the search space, i.e., a space with a more substantial amount of possible values, they are capable of better exploring it, thus, leading to better convergence rates and fitness values. Moreover, as OCS encodes a higher-dimensional space, i.e., 8 dimensions, it was able to achieve the lowest fitness for two datasets (Phishing and Segment), thus showing its exploration capability of the search space.
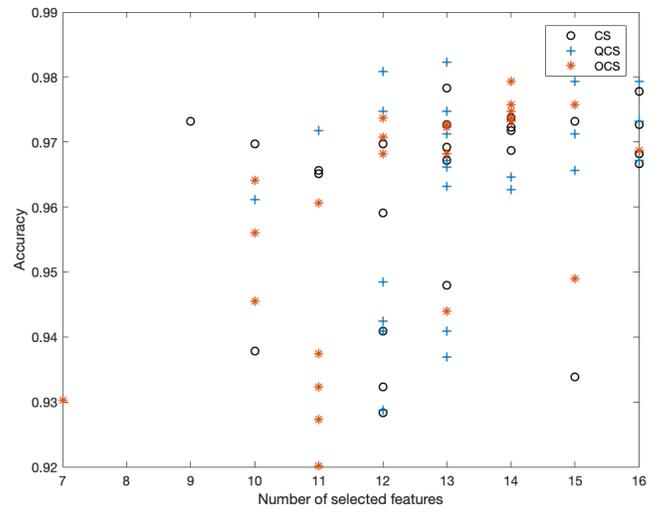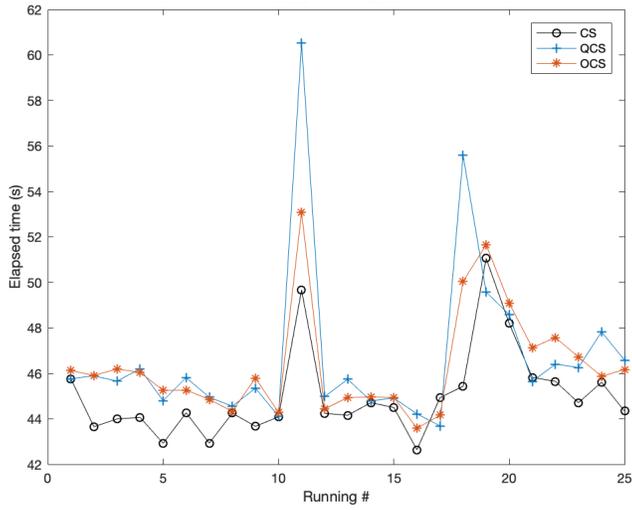
Figure 5: Number of selected features x Accuracy ([0,1]) chart considering CS, QCS and OCS in: (a) DNA, (b) NTL-Commercial, (c) Phishing and (d) Segment datasets.

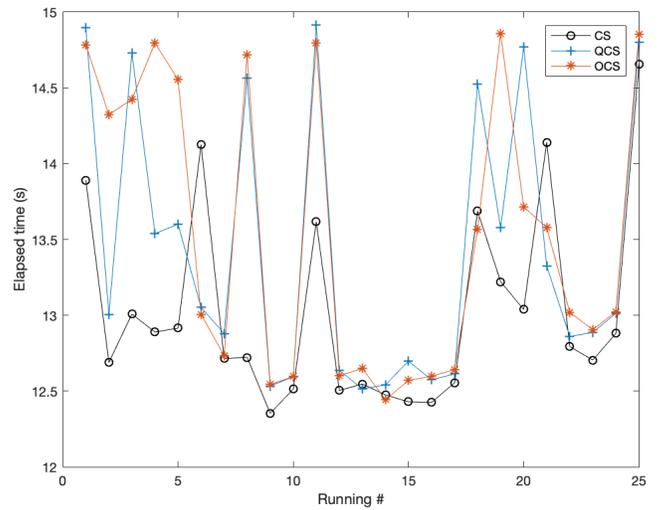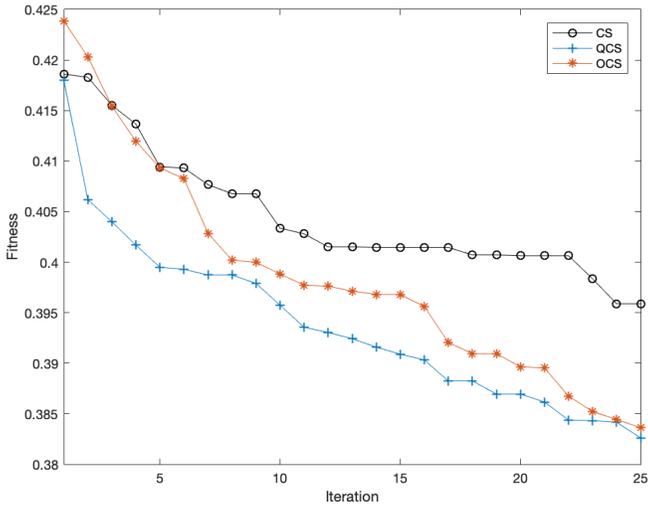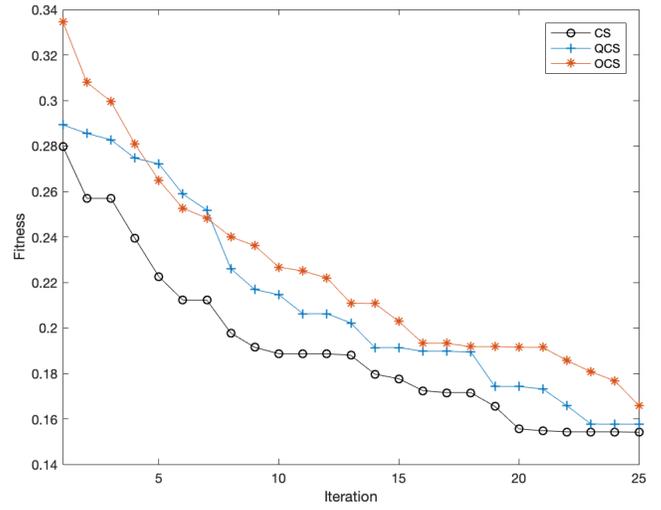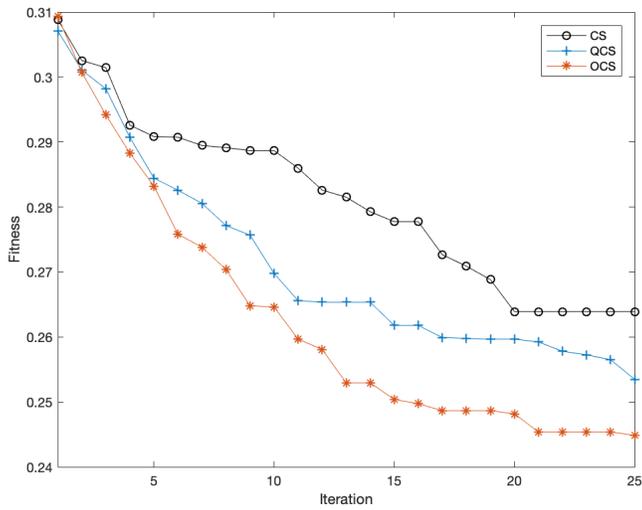Figure 6: Computation time (s) for each independente run of CS, QCS and OCS in: (a) DNA, (b) NTL-Commercial, (c) Phishing and (d) Segment datasets.
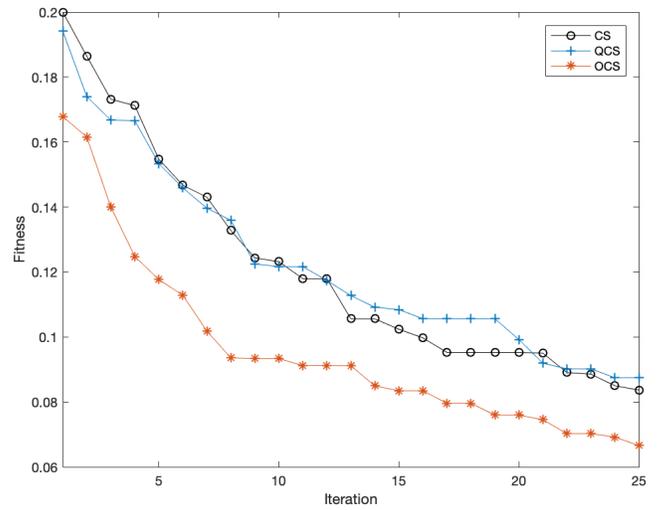
Figure 7: Iteration x Fitness chart considering CS, QCS and OCS in: (a) DNA, (b) NTL-Commercial, (c) Phishing and (d) Segment datasets.

6 Conclusion

This paper addressed the problem of feature selection through a meta-heuristic optimization approach. A wide range of meta-heuristic techniques was employed in 20 distinct datasets in order to provide a more thoughtful numerical validation of the proposed computational framework. Additionally, we also present three distinct search spaces for each optimization technique: standard, quaternionic, and octatonic.

In most circumstances, the meta-heuristic techniques were able to outperform the baseline approach (OPF classification over the full-features dataset). In such cases, outperforming means that a singular technique was able to attain higher accuracy than another algorithm, according to the Wilcoxon signed-rank test with 5% of significance. Besides, it is possible to highlight that all meta-heuristic techniques were able to diminish a substantial number of the initial datasets' features while maintaining their classification accuracy.

Even though most algorithms were able to reduce the features' space size and obtain statistically similar accuracy within respect to the baseline method, in some cases, they reached a slightly lower accuracy than the original OPF classification. Nevertheless, it should be remarked that in the BASEHOCK dataset, where the baseline classification achieved the best accuracy, all other meta-heuristic techniques could decrease by about 35% of the number of features while scoring 2-3% lower accuracy than OPF.

An intriguing fact is that CS was able to obtain the lowest number of features in nearly every dataset, but not necessarily the best accuracy. If one perceives the discrepancy between the best and the worst accuracy considering all datasets (except NTL-based ones) and meta-heuristic techniques, there is not a single one that exceeds the 4.77% limit. Nonetheless, CS underwent in the NTL datasets (energy theft identification), which are highly unbalanced and have a comparatively small amount of features. As CS obtained the lowest number of features in such a low-dimensional dataset, it is reasonable to mention that is has overfitted the optimization process in an attempt to find the lowest number of possible features. Such a procedure penalized the classifier and, consequently, achieved a not proper accuracy for these particular datasets.

Furthermore, we presented a more in-depth analysis considering CS and its variants, QCS, and OCS, among four distinct datasets that have discrepant data, i.e., datasets with a low amount of features and highly sensitive to feature selection. This analysis provided thoughtful insights regarding the number of selected features per accuracy they were able to achieve, the time they took to perform the optimization process, and their convergence process. Additionally, it is essential to highlight that CS hypercomplex-based approaches took more time than their standard version, while they were able to converge better (to a lower fitness function value) than its naïve version.

For future works, we aim at exploring within more depth the hypercomplex mapping function, e.g., norm function. We have high hopes in understanding more the hypercomplex structure, as it seems that one of the central concepts in applying them to feature selection methods lies in transferring values from hypercomplex- to real-valued search spaces.

Acknowledgments

References

[1] X.-S. Yang. *Engineering Optimization: An Introduction with Metaheuristic Applications*. Wiley Publishing, 1st edition, 2010.

[2] B. K. Oh, K. J. Kim, Y. K.and H. S. Park, and H. Adeli. Evolutionary learning based sustainable strain sensing model for structural health monitoring of high-rise buildings. *Applied Soft Computing*, 58:576–585, 2017.

[3] S. Klein, M. Staring, and J. Pluim. Evaluation of optimization methods for nonrigid medical image registration using mutual information and b-splines. *IEEE Transactions on Image Processing*, 16(12):2879–2890, 2007.

[4] N. Dey, S. Samanta, S. Chakraborty, A. Das, S. Chaudhuri, S. Sheli, and J. Suri. Firefly algorithm for optimization of scaling factors during embedding of manifold medical information: an application in ophthalmology imaging. *Journal of Medical Imaging and Health Informatics*, 4(3):384–394, 2014.

[5] G. H. Rosa, J. P. Papa, A. N. Marana, W. Scheirer, and D. D. Cox. Fine-tuning convolutional neural networks using harmony search. In *Progress in Pattern Recognition, Image Analysis, Computer Vision, and Applications*. Springer International Publishing, 2015.

[6] J. P. Papa, G. H. Rosa, K. A. P. Costa, A. N. Marana, W. Scheirer, and D. D. Cox. On the model selection of Bernoulli restricted Boltzmann machines through harmony search. In *Proceedings of the Genetic and Evolutionary Computation Conference*, GECCO '15, pages 1449–1450, New York, USA, 2015. ACM.

[7] J. P. Papa, W. Scheirer, and D. D. Cox. Fine-tuning deep belief networks using harmony search. *Applied Soft Computing*, 46:875–885, 2016.

[8] J. P. Papa, G. H. Rosa, A. N. Marana, W. Scheirer, and D. D. Cox. Model selection for discriminative restricted Boltzmann machines through meta-heuristic techniques. *Journal of Computational Science*, 9:14–18, 2015.

[9] D. P. Bertsekas. *Nonlinear Programming*. Athena Scientific, Belmont, 1999.

[10] X. M. Hu, J. Zhang, Y. Yu, H. S. H. Chung, Y. L. Li, Y. H. Shi, and X. N. Luo. Hybrid genetic algorithm using a forward encoding scheme for lifetime maximization of wireless sensor networks. *IEEE Transactions on Evolutionary Computation*, 14(5):766–781, 2010.

[11] W. N. Chen, J. Zhang, Y. Lin, N. Chen, Z. H. Zhan, H. S. H. Chung, Y. Li, and Y. H. Shi. Particle swarm optimization with an aging leader and challengers. *IEEE Transactions on Evolutionary Computation*, 17(2):241–258, 2013.

[12] E. Pitzer and M. Affenzeller. *A Comprehensive Survey on Fitness Landscape Analysis*. Springer, Berlin, 2012.

[13] R. Kohavi and G. H. John. Wrappers for feature subset selection. *Artificial Intelligence*, 97(1-2):273–324, 1997.

[14] N. Sánchez-Maroño, A. Alonso-Betanzos, and M. Tombilla-Sanromán. Filter methods for feature selection–a comparative study. In *International Conference on Intelligent Data Engineering and Automated Learning*, pages 178–187. Springer, 2007.

[15] I. Fister, X.-S. Yang, J. Brest, and I. Fister Jr. Modified firefly algorithm using quaternion representation. *Expert Systems with Applications*, 40(18):7220–7230, 2013.

[16] I. Fister, J. Brest., I. Fister Jr., and X.-S. Yang. Modified bat algorithm with quaternion representation. In *IEEE Congress on Evolutionary Computation*, pages 491–498, 2015.

[17] J. P. Papa, D. R. Pereira, A. Baldassin, and X.-S. Yang. On the harmony search using quaternions. In F. Schwenker, H. M. Abbas, N. El-Gayar, and E. Trentin, editors, *Artificial Neural Networks in Pattern Recognition: 7th IAPR TC3 Workshop, ANNPR*, pages 126–137, Cham, 2016. Springer International Publishing.

[18] J. P. Papa, G. H. Rosa, D. R. Pereira, and X.-S. Yang. Quaternion-based deep belief networks fine-tuning. *Applied Soft Computing*, 60:328–335, 2017.

[19] J. C. Hart, G. K. Francis, and L. H. Kauffman. Visualizing quaternion rotation. *ACM Transactions on Graphics (TOG)*, 13(3):256–276, 1994.

[20] J. T. Graves. On a connection between the general theory of normal couples and the theory of complete quadratic functions of two variables. *Philosophical Magazine*, 26(173):315–320, 1845.

[21] S. De Leo. Quaternions and special relativity. *Journal of Mathematical Physics*, 37(6):2955–2968, 1996.

[22] D. Finkelstein, J. M. Jauch, S. Schiminovich, and D. Speiser. Foundations of quaternion quantum mechanics. *Journal of Mathematical Physics*, 3(2):207–220, 1962.

[23] D. Eberly. Quaternion algebra and calculus. Technical report, Magic Software, 2002.

[24] J. P. Papa, A. X. Falcão, and C. T. N. Suzuki. Supervised pattern classification based on optimum-path forest. *International Journal of Imaging Systems and Technology*, 19(2):120–131, 2009.

[25] J. P. Papa, A. X. Falcão, V. H. C. Albuquerque, and J. M. R. S. Tavares. Efficient supervised optimum-path forest classification for large datasets. *Pattern Recognition*, 45(1):512–520, 2012.

[26] João Paulo Papa, Gustavo Henrique de Rosa, and Xin-She Yang. *On the Hypercomplex-Based Search Spaces for Optimization Purposes*, pages 119–147. Springer International Publishing, Cham, 2018.

[27] M. Hollander, D. A. Wolfe, and E. Chicken. *Nonparametric Statistical Methods*, volume 751. John Wiley & Sons, Hoboken, NJ, USA, 2013.

[28] F. Wilcoxon. Individual comparisons by ranking methods. *Biometrics Bulletin*, 1(6):80–83, 1945.

[29] D. Karaboga and B. Basturk. A powerful and efficient algorithm for numerical function optimization: Artificial bee colony (ABC) algorithm. *Journal of Global Optimization*, 39(3):459–471, 2007.

[30] M. M. Ebadzadeh A. Nickabadi and R. Safabakhsh. A novel particle swarm optimization algorithm with adaptive inertia weight. *Applied Soft Computing*, 11:3658–3670, 2011.

[31] X.-S. Yang and A. H. Gandomi. Bat algorithm: a novel approach for global engineering optimization. *Engineering Computations*, 29(5):464–483, 2012.

[32] X-S. Yang and S. Deb. Engineering optimisation by cuckoo search. *International Journal of Mathematical Modelling and Numerical Optimisation*, 1:330–343, 2010.

[33] X.-S. Yang. Firefly algorithm, stochastic test functions and design optimisation. *International Journal Bio-Inspired Computing*, 2(2):78–84, 2010.

[34] S.-S. Yang, M. Karamanoglu, and X. He. Flower pollination algorithm: A novel approach for multiobjective optimization. *Engineering Optimization*, 46(9):1222–1237, 2014.

[35] J. Kennedy and R. C. Eberhart. *Swarm Intelligence*. Morgan Kaufmann Publishers Inc., San Francisco, USA, 2001.